Surface etching of InP(100) by chlorine

Wei-Hsiu Hung [a],*, Jyh-Tsung Hsieh [b], Huey-Liang Hwang [b], Hsin-Yen Hwang [c],
Che-Chen Chang [c]

[a] *Synchrotron Radiation Research Center, Science-Based Industrial Park No. 1, R&D Road VI, Hsin-Chu 30077, Taiwan, ROC*
[b] *Department of Electrical Engineering, National Tsing-Hwa University, Hsin-Chu 30077, Taiwan, ROC*
[c] *Department of Chemistry, National Taiwan University, Taipei 10764, Taiwan, ROC*

Abstract

The cleaning and etching of the InP(100) surface by chlorine gas is investigated using synchrotron-radiation photoemission spectroscopy. A clean InP surface with a 4×2 configuration is obtained by ion sputtering or chlorine etching, followed by annealing to 650 K. The clean surface obtained by chlorine etching and annealing is indium-rich with the surface indium atoms showing metallic characterics. The chemisorption of chlorine leads to the formation of various $InCl_x$ ($x = 1$–3) and PCl species on the InP surface at 110 K and their corresponding chemical shifts are assigned. The chlorination of the InP surface causes surface band bending by about 0.36 eV at the saturation coverage. Argon-ion sputtering enhances the surface reactivity so that the sputtered surface can be chlorinated to a higher extent than the clean surface. © 1998 Elsevier Science B.V. All rights reserved.

Keywords: Chlorine; Etching; InP; Synchrotron-radiation photoelectron spectroscopy

1. Introduction

InP is an important III–V material in electronics applications because of several advantageous properties. Compared with GaAs, InP has higher peak and saturation electron velocity, higher breakdown voltage, larger intervalley energy gap, smaller ionization coefficient and dielectric constant [1]. When reacted with chlorine, most III–V materials form chlorides on the surface, which are volatile at relatively low temperatures. Therefore, chlorine-based etching is often used in the fabrication of devices based on III–V substrates [2,3]. Whether or not the device has the desired characteristics is determined by the quality of the substrate surface, which influences the nature of the interface in the subsequent fabrication process [4]. Understanding in detail the chemical reaction of the InP surface with chlorine has appreciable technological importance in better handling of this material.

Among the different crystal faces, the InP(100) surface is the most important face with respect to its application in optoelectronic devices. However, similar to the GaAs(100) surface, the InP(100) surface can be reconstructed into several configurations in a complex way [5,6]. It is now well known that ion bombardment and heating result in an indium-rich surface [1,7,8]. Depending on the annealing temperature, there are two surface reconstructions that can be observed for the indium-rich surface [9,10]. The InP(100) surface

* Corresponding author. Fax: + 886-3-5783892;
e-mail: whung@alpha1.srrc.gov.tw.

is sufficiently ordered to exhibit a (4×2) low-energy electron diffraction (LEED) pattern after argon-ion bombardment and gentle annealing. In spite of various structures proposed in previous studies, the detailed structure of the InP(100)-4×2 surface is still unclear [6]. Based on the model proposed for the surface structure of GaAs(100), a qualitative missing-row-dimer (MRD) structure has been discussed for the InP(100)-4×2 surface [11–13]. It has been suggested that the surface is covered by some metallic indium atoms [1,14]. The presence of metallic indium atoms on the InP surface may be crucial for obtaining the desired quality of interface for further fabrication [15]. In this study, X-ray photoelectron spectroscopy (XPS) is used to elucidate the nature of the InP(100)-4×2 surface and its reaction with Cl_2.

Furthermore, in contrast to GaAs, a remote chlorine plasma does not etch InP efficiently at temperatures below 125°C [16,17]. It is concluded that the difference in volatility of the etch products gives rise to the differences in both the etching threshold temperature and the temperature dependence of the etching rate for GaAs and InP. A previous temperature-programmed desorption (TPD) study of the chlorinated InP surface showed that the two desorption peaks (α and β states) of InCl and P_4 are observed at 410 and 570 K during thermal desorption [18]. The populations of α and β states are very sensitive to the structure and stoichiometry of the surface. This investigation of the reaction of the InP surface with Cl_2 may provide a better understanding of the difference in etching rates of chlorine between the GaAs and InP surfaces.

Energetic ions have been used to enhance the etching rate of various material surfaces [19]. Argon-ion beams are extensively used for ion-assisted dry etching of semiconductors because of their chemical inertness and high sputtering yield [20]. On the other hand, the chemical and physical damage on the surface after reactive-ion etching (RIE) may cause undesirable surface properties. The damage can be reduced by a post-RIE process or removed through a thermal reaction with chlorine, which generates volatile chlorides [21]. Thus it is of considerable importance to study in detail the effect of ion bombardment on the interaction of the InP surface with chlorine gas.

Chlorine is also used in the low-temperature RIE process to obtain a less-damaged etched InP surface with good anisotropy and smooth stoichiometry [22]. Since Group III and V chlorides are volatile, they may desorb from the surface after being formed during Cl_2 exposure, without resorting to a vigorous thermal treatment. Therefore, when the InP is etched, the substrate temperature can be kept low so that the chlorides formed on the surface of the side wall can remain intact for better anisotropic etching profile [23]. The advantage of etching at low temperatures also includes the fact that the sticking coefficient of Cl_2 on the InP surface is increased at low temperature. All the experiments in this study were thus performed by cooling the InP sample with liquid nitrogen to 110 K. Results obtained from the low-temperature study may provide clues to the fundamental surface chemistry of chlorine etching, which may eventually help in process design.

2. Experimental

Experiments were performed in an ultrahigh vacuum (UHV) chamber equipped with a quadrupole mass spectrometer, a low-energy electron diffractometer and a VG CLAM II electron-energy analyzer. The XPS measurements were carried out at the 6 m LSGM beamline of SRRC (Synchrotron Radiation Research Center, Taiwan). The incident angle of photons was 55° from the surface normal. The emitted photoelectrons were collected with the electron analyzer normal to the sample surface. The InP sample was mounted on the tantalum plate by indium bonding, to achieve good contact. The sample can be cooled to 110 K with liquid nitrogen and heated by electron beam bombardment from the back of the tantalum plate. The surface temperature was measured by using a K-type thermocouple spot-welded close to the sample. The InP(100) sample (S-doped n-type, $\sim 3 \times 10^{18}$ cm^{-3}) was cleaned by chemical etching using sulfuric acid and hydrogen peroxide solution. The etched InP sample was rinsed in deionized water and was cleaned by argon-ion bombardment

(500 eV) with the ion beam at a 45° incident angle in UHV. Following Ar^+-ion bombardment, the sample was annealed to ~650 K for 2 min. A 4 × 2 LEED pattern was observed, which is characteristic of an indium-rich InP(100) surface. For exposure of the sample to Cl_2, the chlorine gas was introduced to the InP(100) surface by background dosing through a leak valve.

All XPS spectra were taken at a sample temperature of 110 K. The spectra collected were fitted numerically with Gaussian-broadened Lorentzian spin–orbit doublets after Shirley background subtraction with a third-order polynomial to each side of the peak in all fits [24]. The Lorentzian full-width at half-maximum (FWHM) was fixed at 0.15 eV for In 4d and 0.10 eV for P 2p. The peak width of each core-level component is mainly determined by the Gaussian FWHM. The spin–orbit splitting values are 0.85 eV for In 4d and 0.86 eV for P 2p.

3. Results and discussion

Fig. 1 shows the core-level spectra of In 4d and P 2p for the InP(100) surface sputtered by 500 eV Ar^+ ions for 30 min and then annealed to 650 K. The photon energy used to collect these spectra is 50 eV for In 4d and 160 eV for P 2p. Photoelectrons from In 4d and P 2p are all measured at about 30 eV. Thus, the analyzing depth of the InP substrate for both the In 4d and P 2p spectra is about the same.

The assignments of the XPS spectra for the clean InP(100)-4 × 2 surface are necessary for the interpretation of the chemical species formed on the InP surface upon the adsorption of chlorine. The indium spectra are best fitted with the branching ratio of 0.68 ± 0.02. From our curve fitting, the XPS spectrum of a clean InP(100)-4 × 2 surface shows several indium chemical components with the 4$d_{5/2}$ binding energies at 16.92, 17.27, 17.67 and 17.86 eV, as shown in Fig. 1. The peak with a binding energy at 17.67 eV is obtained due to the contribution from the bulk InP. The peaks with binding energies at 16.92, 17.27 and 17.86 eV are attributed to metallic indium atoms and indium adatoms with dangling bonds (S1 and S2) on the
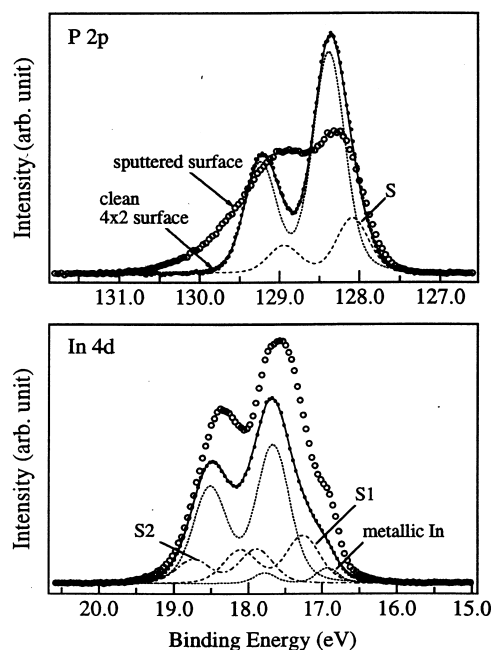

Fig. 1. Soft X-ray photoelectron spectra of In 4d and P 2p, collected from an InP(100) surface after the sample had been either bombarded by 500 eV Ar^+ ions for 30 min or sputtered and annealed to 650 K. The photon energy used to collect these spectra is 50 eV for the In 4d level and 160 eV for the P 2p level. The dots represent the data collected after background subtraction, the solid line is the curve fit to the data, and the various components are shown by dashed lines. The surface-shifted core-level components of indium and phosphorus are labeled S1, S2 and S, respectively.

surface, respectively. A Gaussian FWHM of 0.27 ± 0.02 eV is used for the metallic indium atoms in all In 4d spectra. This width is significantly smaller than that obtained for bulk and surface indium (0.45 ± 0.02 eV). The value of the Gaussian FWHM for the metallic indium component is obtained from a well-resolved spectrum of the chlorinated InP surface which is to be discussed later. The P 2p spectrum can be fitted well with a branching ratio of 0.50 ± 0.01 for $p_{1/2}$ and $p_{3/2}$, and the binding energy of the surface core-level component is shifted from that of the bulk by −0.31 eV.

The intensities of In 4d and P 2p for the clean and sputtered surfaces, shown in Fig. 1, are normalized to the photon flux. For the sputtered surface, there is an increase in the intensity at the low-binding-energy side of the In 4d spectrum,

whereas a broad tail appears at high binding energy in the P 2p spectrum. There has been some dispute over the composition of a sputtered InP surface [1,10,25–29]. We make no attempt to deconvolute the spectra of a sputtered InP surface because of the complication of the surface composition (stoichiometry of indium and phosphorus) and roughness due to the energetic-ion bombardment. The long tail of P 2p at the high-binding-energy side may suggest the presence of InP_x with a phosphorus-rich stoichiometry or phosphorus adatoms on the sputtered and roughened surface, which has higher binding energy than the bulk phosphorus atoms.

In this study, a 4×2 LEED pattern with large, weak half-order spots is obtained on the clean InP(100) sample after argon-ion sputtering and annealing to 650 K. This suggests that the clean InP surface obtained in this study is not perfectly ordered. Its surface geometry may be considered as a 4×2 structure, on which the $c(8 \times 2)$ structure is present [11,30,31]. The metallic indium clusters may be present on the surface and thus hinder the complete reconstruction of the $c(8 \times 2)$ structure [32]. This surface structure is expected to be the most stable structure on the (100) III–V semiconductor surface at high temperatures, and has been observed on the GaAs(100) surface before [33,34]. In addition, the LEED pattern obtained reveals that the area of the ordered surface domains may be close to or less than the coherence width (~ 100 Å) of the electron beam source used in the LEED experiment [35]. Metallic indium clusters may thus be somewhat randomly distributed on the surface at a distance which, on average, is less than the coherence width.

Figs. 2 and 3 show the XPS spectra for In $4d_{5/2}$ and P 2p of an InP(100)-4×2 surface exposed to various amounts of chlorine at 110 K. For simplicity and clarity, only the $4d_{5/2}$ component obtained from deconvolution of the experimental data is presented in Fig. 2 for the In $4d$ spectra [36]. As evident from the significant changes in both the In $4d$ and P 2p spectra with chlorine exposure, chlorination occurs on both the indium and phosphorus atoms upon the adsorption of chlorine. The chlorine-induced components appear at high binding energy, which is indicative of the forma-
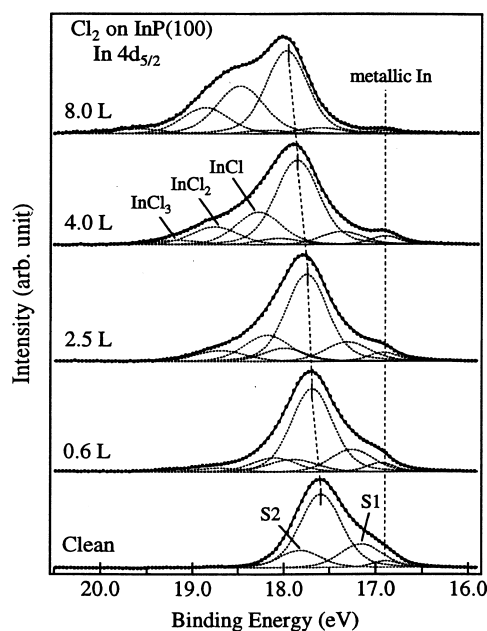

Fig. 2. Soft X-ray photoelectron spectra of In $4d_{5/2}$ from the InP(100)-4×2 surface with various exposures to Cl_2 at 110 K.
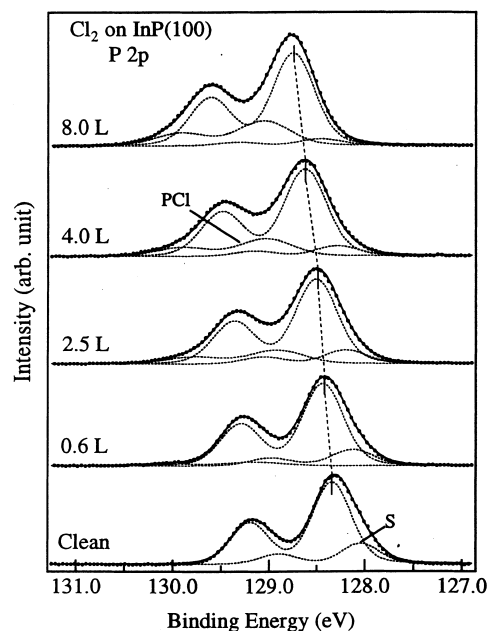

Fig. 3. Soft X-ray photoelectron spectra of P 2p from the InP(100)-4×2 surface with various exposures to Cl_2 at 110 K.

tion of indium and phosphorus chlorides. From our data fitting, the chemical shifts of indium chlorides with respect to that of the bulk InP are 0.44, 0.86 and 1.36 eV. These shifts are attributed to the formation of InCl, $InCl_2$ and $InCl_3$ on the surface. For the phosphorus components, as shown in Fig. 3, only a PCl species is formed on the surface upon chlorine adsorption. This species has a chemical shift of 0.34 eV from the bulk InP. The intensities of the peaks due to the clean surface indium and phosphorus atoms decrease with increasing Cl_2 exposure. The chlorination of InP(100) is saturated when the surface is exposed to chlorine of more than 10 L at 110 K. At higher exposures, a passivation layer of indium and phosphorus chlorides is formed, and molecular chlorine physisorbs and accumulates on the surface.

With the increase of Cl_2 exposure, the peaks assigned to bulk In $4d$ and P $2p$ shift to higher binding energies than that of the clean surface. The shift of the bulk indium and phosphorus components relative to the spectra of the clean surface is due to the occurrence of the surface band bending, which induces a change in the binding energy of the core level relative to the Fermi level [36]. The chemisorption of chlorine with strong electronegativity may cause a change in the electrostatic potential and result in a shift of the core level of the bulk InP to higher binding energy. The surface band bending increases with the extent of chlorination, i.e., the exposure to chlorine. On the chlorine-saturated InP surface, the binding energies of the bulk In $4d$ and P $2p$ are lifted by about 0.36 eV from the clean InP(100)-4×2 surface. It was reported that the adsorption of Cl_2 on a cleaved InP(110) surface caused a downshift of the Fermi level by 0.2–0.3 eV from the conduction band [15]. The binding energy of the component assigned to metallic indium remains essentially unchanged on the chlorinated surface. This suggests that the metallic indium atoms, however, remain as clusters on the InP surface and act as individual systems. These clusters are not affected by the average electrical field felt by the indium and phosphorus atoms in the bulk and surface InP.

To achieve a good fitting of the collected In $4d$ and P $2p$ spectra from the chlorinated InP surface, it is necessary to include the components with shifts in binding energies from the substrate peak of -0.4 and 0.2 eV for the indium atom and -0.32 eV for the phosphorus atom. These shifts in binding energy are due to the presence of adatoms with dangling bonds on the clean surface, which persist on the surface with saturated chlorination. Similar persistence of these components was also observed for the GaAs surfaces exposed to XeF_2 and to Cl_2 [37,38]. They were attributed to the gallium and arsenic atoms generated on the substrate with a tri-coordinated configuration as a result of the bond breaking during halogenation, which have similar binding energy shifts as the surface-induced chemical shifts. During chlorination, the bond breaking of In–P occurs at the interface between the bulk and the chloride layer. Consequently, the tri-coordinated atoms are created and the chloride layer grows. At a Cl_2 exposure of more than 10 L, the thick indium and phosphorus chloride layer may become passivated, and chlorine cannot react further with bulk InP and tri-coordinated atoms.

The intensities of surface components decrease with increasing chlorine exposures. At initial chlorination, the intensity of the surface indium adatoms (S1 and S2) in In $4d$ spectra decreases more drastically than that of the metallic indium atoms. During this time, most of the adsorbed chlorine reacts with the surface indium adatoms to form indium chlorides. This is consistent with the argument that the metallic indium atoms concentrate in droplets, rather than in a continuous film, and cover a small fraction of the surface area. Since some metallic indium atoms can persist even at the saturation coverage, the indium atoms inside the droplet may be relatively inert to further chlorination after a chlorinated passivation layer on the outside is formed at a temperature as low as 110 K.

Indium and phosphorus chlorides are observed on the InP surface at low exposures of chlorine, and there is no obvious preference of the chlorination with either surface indium or phosphorus atoms. Among the indium chlorides, InCl and $InCl_2$ are the main products and only a small amount of $InCl_3$ is formed. PCl is the only product of the phosphorus chlorides. However, by compar-

ing the chloride intensity to the bulk intensity, it is found that the chlorinated InP surface is mainly composed of indium chlorides. The preferential formation of indium chlorides upon chlorine adsorption may result from the domination of the indium atoms on the clean InP surface. This suggests that the clean InP surface is mainly covered by the indium atoms, as described above.

Figs. 4 and 5 show the XPS spectra of In $4d_{5/2}$ and P $2p$ for an InP(100)-4×2 surface exposed to 8 L Cl_2 at 110 K, followed by warming up to the indicated temperatures. When the substrate is heated up to 250 K, the intensity of the metallic indium atoms at 16.92 eV is diminished while the intensity of indium chlorides increased. This suggests that the metallic indium clusters can be decomposed by further reacting with the physisorbed chlorine to form more indium chlorides upon thermal annealing. When the surface is heated up to 400 K, $InCl_3$ is completely depleted and a small amount of InCl and $InCl_2$ desorbs from the surface. A well-resolved peak at 16.9 eV
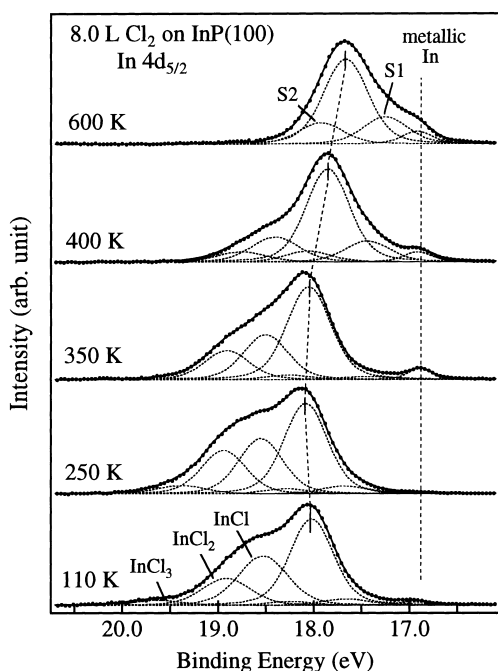
Fig. 4. Soft X-ray photoelectron spectra of In $4d_{5/2}$ from the InP(100) surface exposed to 8 L Cl_2 at 110 K, followed by annealing the substrate to 250 K, 350 K or 400 K.
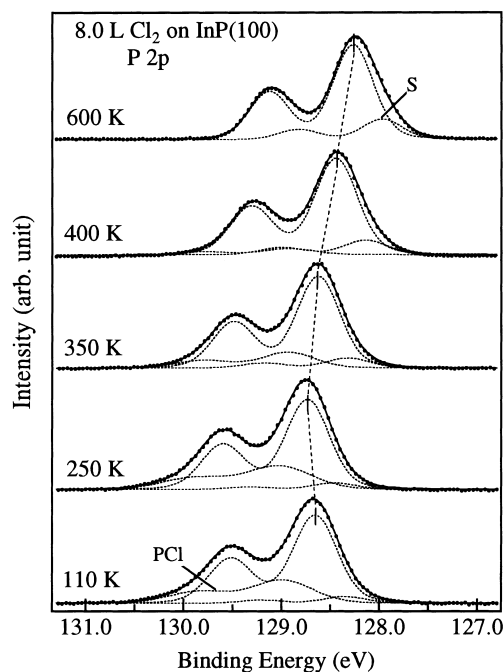
Fig. 5. Soft X-ray photoelectron spectra of P $2p$ from the InP(100) surface exposed to 8 L Cl_2 at 110 K, followed by annealing the substrate to 250 K, 350 K or 400 K.

is observed at 350 K with a Gaussian FWHM of 0.27 eV, which is smaller than that of bulk InP. It has been also observed that large metallic indium droplets exist on the heavily hydrogenated InP surface [14,39–41]. The FWHM of the metallic In $4d$ peak is smaller than in bulk InP due to the difference of their bonding character. Fig. 4 thus indicates that the metallic indium droplets reappear on the surface during the desorption of indium chlorides. The FWHM of the peak at 16.9 eV is used in the curve fitting of the metallic indium component in all In $4d$ spectra.

When the surface is annealed to 600 K, all indium and phosphorus chlorides desorb from the surface and a blurred InP(100)-4×2 surface is recovered, like that obtained by ion bombardment and annealing. The surface band bending is reduced when the sample is heated to desorb surface chlorides. The regeneration of the clean surface is thus accomplished by thermal desorption of surface indium and phosphorus chlorides. The results indicate that, when the substrate is annealed

above 600 K, the indium-rich surface covered with metallic indium atoms is the favorable configuration thermodynamically.

The XPS spectra shown in Figs. 4 and 5 suggest that the desorption of surface chlorides from the chlorinated InP surface occurs over a very wide temperature range. It may consist of more than one desorption stage. In a previous TPD study, it was found that the desorption was a two-stage process including α and β states [20]. The desorption of the α state started at ~ 350 K and the β state desorbed at ~ 500 K. Two phases of chlorides may thus be present on the surface. The α state was attributed to the chemisorbed adlayer and the β state the bulk corrosion phase. It also showed that the population of these two states is strongly dependent on the preparation of the InP surface. Bombardment of the InP surface with Ar^+ ions resulted in an increase of the α state. This study shows that, since the bombardment induces the formation of metallic indium as described above, the α state may be attributed to the indium chlorides formed due to the reaction of metallic indium with chlorine. The β state may be attributed to a mixed phase of indium and phosphorus chlorides, which is formed from the reaction of both the surface and the bulk InP with chlorine. This assignment is in contrast to the previous one [20]. Since the clean surface, which is an indium-rich surface containing indium droplets, can be obtained after annealing the chlorinated surface to 600 K, desorption of surface phosphorus atoms must have occurred during the thermal annealing after chlorides desorb. In fact, it was found that P_4, instead of PCl, was the desorption product of phosphorous species in the thermal desorption, and its desorption temperature was marginally higher than that of indium chlorides [20]. This implies that, during the thermal annealing, the chlorine atoms in PCl are transferred to the indium atoms nearby to form gaseous indium chlorides. The phosphorus atoms left on the surface thus desorb to restore a surface stoichiometry of indium enrichment, which is thermodynamically stable. The desorption of indium chlorides, rather than phosphorus chloride, may be due to the stronger bonding energy of In–Cl ($E_{dis} = 4.5$ eV) than that of P–Cl ($E_{dis} = 3.0$ eV) [42].

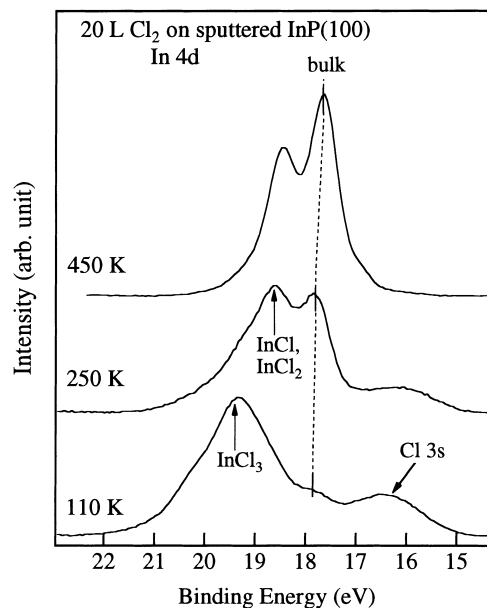Figs. 6 and 7 show In $4d$ and P $2p$ spectra taken

Fig. 6. Soft X-ray photoelectron spectra of In $4d_{5/2}$ from the sputtered InP(100) surface exposed to 20 L Cl_2 at 110 K, followed by annealing the substrate to 250 K or 450 K.
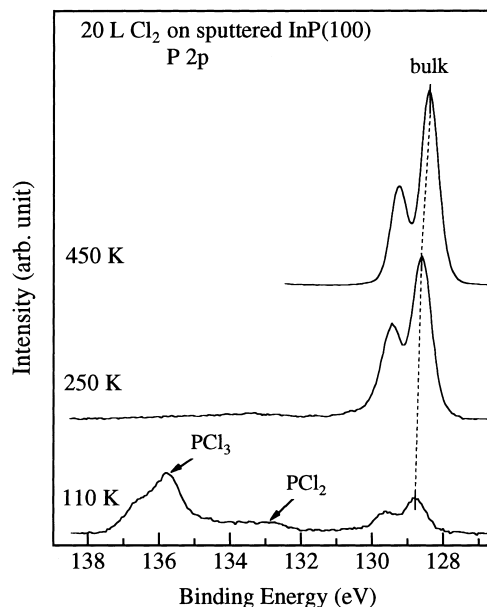

Fig. 7. Soft X-ray photoelectron spectra of P $2p$ from the sputtered InP(100) surface exposed to 20 L Cl_2 at 110 K, followed by annealing the substrate to 250 K or 450 K.

from a bombarded InP surface which was exposed to 20 L Cl_2 at 110 K, followed by being annealed to 250 K or 450 K. Upon the adsorption of chlorine on the bombarded surface, the intensities of bulk indium and phosphorus are attenuated by the thick indium and phosphorus chloride layer. Fig. 6 shows that a large amount of $InCl_3$ is formed on the bombarded surface. This is in contrast to that observed from the sputtered and annealed surface on which $InCl_2$ and InCl dominate after chlorination. There is a broad peak centered at about 16.5 eV, which is due to the Cl 3s. The intensity of Cl 3s decreases upon the desorption of surface chlorides by thermal annealing. Fig. 7 shows that, in addition to the PCl formation, PCl_2 and PCl_3 are formed on the bombarded InP surface upon the adsorption of chlorine. The binding energies of P 2p in PCl_2 and PCl_3 are higher than that in bulk InP by 3.9 eV and 7.1 eV, respectively. It appears that the reactivity of the surface is promoted by ion bombardment to form higher chlorinated species. The saturation exposure of Cl_2 on the bombarded surface is also higher than that on the annealed surface. Compared with the sputtered and annealed surface, more indium and phosphorus chlorides are formed on the bombarded InP surface at saturated chlorination. The increase in the reactivity of the bombarded surface is not due to ion implantation of argon. It is known that, after ion bombardment, argon is trapped in the InP substrate as an interstitial impurity with low equilibrium concentration [43]. The chemical affinity between argon and InP is so small that the increased reactivity of the bombarded surface should be mainly due to the surface inhomogeneity. The Ar^+-ion bombardment results in a roughened InP surface and generates inhomogeneity in the surface composition and structure. The damaged surface may consist of adatoms which exist in a configuration with dangling bonds or in a looser bonding structure. They are thus more reactive to chlorine and can be highly chlorinated.

Figs. 6 and 7 show that $InCl_3$, PCl_2 and PCl_3 species desorb from the surface after heating the substrate to 250 K. However, $InCl_2$, InCl and PCl can still remain on the surface, as observed in the experiments performed on the sputtered and annealed surface. As described above, the ion bombardment can increase the surface reactivity with chlorine to form highly chlorinated indium and phosphorus species ($InCl_3$, PCl_2 and PCl_3). These chlorides are highly volatile and readily desorb from the surface at temperature below 250 K. As a consequence, bombardment of the sample may enhance the etching rate of InP by chlorine to some degree. In this case, the etching rate may be more or less limited by the formation of the highly volatile products (i.e., $InCl_3$, PCl_2, and PCl_3) at low temperatures.

4. Conclusions

The XPS study shows that the InP(100)-4 × 2 surface is an indium-rich surface with the presence of metallic indium atoms. These atoms may exist on the surface in the form of microdroplets and cover only a small fraction of the surface area. Chlorination of the InP(100)-4 × 2 surface causes changes in the surface composition and results in surface band bending. For chlorination to occur on the clean surface, InCl and $InCl_2$ are the major indium chloride and PCl is the only phosphorous chloride upon the adsorption of chlorine. The clean InP surface can be regenerated by thermally annealing the chlorinated surface to 600 K. Ar^+-ion bombardment can create more reactive surface features that can be extensively chlorinated. The etching rate of the InP surface by chlorine may thus be enhanced at low temperature by irradiation of the sample with energetic ions.

Acknowledgements

References

[1] J.B. Malherbe, W.O. Barnard, Surf. Sci. 255 (1991) 309.
[2] T. Yoshikawa, S. Kohmoto, M. Anan, Y. Sugimoto, M.

Sugomoto, K. Asakawa, Jpn J. Appl. Phys. Part 1 31 (1992) 4381.

[3] S.J. Pearton, Mater. Sci. Eng. B 10 (1991) 187.

[4] J. Massies, P. Devoldere, N.T. Linh, J. Vac. Sci. Technol. 15 (1978) 1353.

[5] M. Shimomura, N. Sanada, Y. Fukuda, P.J. Moller, Surf. Sci. 359 (1996) L451.

[6] M.M. Sung, C. Kim, H. Bu, D.S. Karpuzov, J.W. Rabalais, Surf. Sci. 322 (1995) 116.

[7] J. Massies, F. Lemaire-Dezaly, J. Appl. Phys. 57 (1985) 237.

[8] P. Soukiassian, P.S. Mangat, Y. Huttel, Z. Hurych, B. Gruzza, A. Porte, J. Vac. Sci. Technol. B 11 (1993) 1603.

[9] F. Lodders, J. Westhof, J.A. Schaefer, H. Hopfinger, A. Goldmann, S. Witzel, Z. Phys. B 83 (1991) 263.

[10] X. Wang, Appl. Surf. Sci. 33/34 (1998) 88.

[11] X. Hou, G. Dong, X. Ding, X. Wang, J. Phys. C 20 (1987) L121.

[12] C.B. Duke, Appl. Surf. Sci. 65 (1993) 543.

[13] M.M. Sung, J.W. Rabalais, Surf. Sci. 342 (1996) L1137.

[14] J. Woll, T. Allinger, V. Polyakov, J.A. Schaefer, A. Goldmann, W. Erfurth, Surf. Sci. 315 (1994) 293.

[15] V. Montgomery, R.H. Williams, R.R. Varma, J. Phys. C: Solid State Phys. 11 (1978) 1989.

[16] D.G. Lishan, E.L. Hu, J. Vac. Sci. Technol. B 8 (1990) 1951.

[17] S.C. McNevin, J. Vac. Sci. Technol. B 4 (1986) 1203.

[18] A.J. Murrell, R.J. Price, R.B. Jackman, J.S. Foord, Surf. Sci. 227 (1990) 197.

[19] A.T. Demos, H.S. Fogler, H. Etemad-Moghadam, M.E. Elta, J. Electrochem. Soc. 138 (1991) 1143.

[20] R. Behrisch (Ed.), Sputtering by Particles Bombardment II, Springer, Berlin, 1983.

[21] H.C. Duran, R. Cheung, W. Patrick, W. Bachtold, I. Pfund, G. Hahner, Microelectronic Eng. 35 (1997) 67.

[22] G.F. Doughty, S. Thoms, V. Law, C.D.W. Wilkinson, Vacuum 36 (1986) 803.

[23] M.C. Shih, M.B. Freiler, R. Scarmozzino, R.M. Osgood Jr., J. Vac. Sci. Technol. B 13 (1995) 43.

[24] W.C. Simpson, D.K. Shuh, J.A. Yarmoff, J. Vac. Sci. Technol. B 14 (1996) 2909.

[25] X. Jin, M. Yu, X. Wang, Chin. Phys. Lett. 2 (1985) 345.

[26] W.M. Lau, R.N.S. Sodhi, B.J. Flinn, K.H. Tan, G.M. Bancroft, Appl. Phys. Lett. 51 (1987) 177.

[27] C. Jardin, D. Robert, B. Achard, B. Gruzza, C. Pariset, Surf. Interface Anal. 10 (1987) 301.

[28] X. Jin, M. Yu, X. Wang, Chin. Phys. Lett. 7 (1987) 854.

[29] S. Abdellaoui, B. Gruzza, C. Pariset, M. Bouslama, C. Jardin, D. Robert, Surf. Sci. 208 (1989) L21.

[30] O. M'Hamedi, F. Proix, J.P. Lacharme, C.A. Sebenne, Surf. Sci. 199 (1988) 121.

[31] J.M. Moison, M. Bensoussan, J. Vac. Sci. Technol. 21 (1982) 315.

[32] W. Weiss, R. Hornstein, D. Schmeisser, W. Gopel, J. Vac. Sci. Technol. B 8 (1990) 715.

[33] K. Jacobi, W. Ranke, Prog. Surf. Sci. 10 (1981) 1.

[34] P. Drahten, W. Ranke, K. Jacobi, Surf. Sci. 77 (1978) L162.

[35] G.A. Somorjai, Chemistry in Two Dimensions Surface, Cornell University Press, Ithaca, NY, 1981.

[36] F.J. Himpsel, B.S. Meyerson, F.R. McFeely, J.F. Morar, A. Taleb-Ibrahima, J.A. Yarmorff, in: M. Campagna, R. Rosei (Eds.), Photoemission and Absorption Spectroscopy of Solids and Interfaces with Synchrotron Radiation, North-Holland, Amsterdam, 1990.

[37] P.R. Varekamp, W.C. Simpson, D.K. Durbin, V. Chakarian, J.A. Yarmoff, Phys. Rev. B 50 (1995) 14267.

[38] W.H. Hung, S.L. Wu, C.C. Chang, J. Phys. Chem. 102 (1998) 1141.

[39] J.A. Schaefer, F. Stietz, J. Woll, J. Vac. Sci. Technol. 11 (1993) 1497.

[40] F. Stietz, V. Persch, T. Allinger, J.A. Schaefer, G.J. Lapeyre, J. Electron Spectrosc. Relat. Phenom. 64/65 (1993) 413.

[41] F. Stietz, T. Allinger, V. Polyakov, J. Woll, A. Goldmann, W. Erfurth, G.J. Lapeyre, J.A. Schaefer, Appl. Surf. Sci. 104/105 (1996) 169.

[42] D.R. Lide (Ed.), CRC Handbook of Chemistry and Physics, CRC Press, Boca Raton, FL, 1994.

[43] J.S. Pan, A.T.S. Wee, C.H. Huan, H.S. Tan, K.L. Tan, J. Appl. Phys. 80 (1996) 6655.